Electrochimica Acta 541 (2025) 147285

Contents lists available at ScienceDirect

Electrochimica Acta

journal homepage: www.journals.elsevier.com/electrochimica-acta

Trident-shaped fully 3D-printed electrochemical sensor for real-time measurements

Martina Tuccillo [a,1], Panagiota M. Kalligosfyri [a,1,*], Antonella Miglione [a], Concetta Di Natale [b], Michele Spinelli [c], Angela Amoresano [c], Donato Calabria [d,e], Mara Mirasoli [d,e,f], Ibrahim A. Darwish [g], Stefano Cinti [a,h,i,*]

[a] Department of Pharmacy, University of Naples "Federico II", Naples 80131, Italy
[b] University of Naples Federico II, Dipartimento di Ingegneria Chimica, dei Materiali e della Produzione Industriale, P.le Tecchio 80, Naples I-80125, Italy
[c] Department of Chemical Sciences, University of Naples "Federico II", Naples 80126, Italy
[d] Department of Chemistry "Giacomo Ciamician", Alma Mater Studiorum - University of Bologna, Via Piero Gobetti 85, Bologna 40129, Italy
[e] Interdepartmental Centre for Industrial Aerospace Research (CIRI AEROSPACE), Alma Mater Studiorum-University of Bologna, Via Baldassarre Canaccini 12, Forlì I-47121, Italy
[f] Interdepartmental Centre for Industrial Research in Renewable Resources, Environment, Sea and Energy (CIRI FRAME), Alma Mater Studiorum - University of Bologna, Via Sant'Alberto 163, Ravenna I-48123, Italy
[g] Department of Pharmaceutical Chemistry, College of Pharmacy, King Saud University, P.O. Box 2457 Riyadh 11451, Saudi Arabia.
[h] Sbarro Institute for Cancer Research and Molecular Medicine, Center for Biotechnology, College of Science and Technology, Temple University, Philadelphia, PA 19122, USA
[i] Bioelectronics Task Force at University of Naples Federico II, Via Cinthia 21, Naples 80126, Italy

ARTICLE INFO

Keywords:
3D-printed sensors
Additive manufacturing
Conductive PLA
Electrochemical sensor
Ascorbic acid

ABSTRACT

Accurate analysis of fresh fruit and vegetable samples typically relies on complex instrumentation, skilled personnel, and extensive sample preparation, limiting its accessibility for decentralized testing. To overcome these challenges, we developed a fully 3D-printed, trident-shaped electrochemical sensor for direct, in situ detection of target analytes without any sample pre-treatment. The device was fabricated using low-cost, commercially available conductive and insulating filaments, and designed for seamless integration with portable or smartphone-connected potentiostats. The custom trident geometry enabled direct insertion into fruit and vegetable samples, eliminating the need for sample pre-treatment steps. Among tested configurations, rectangular working electrodes printed with simple infill patterns at 70 % printing speed exhibited optimal electrochemical performance, underscoring the critical impact of electrode design and printing parameters on sensor response. Linear sweep voltammetry was selected for its simplicity, rapid data acquisition, and compatibility with field-based applications. As a proof of concept, the sensor was used to quantify ascorbic acid in fresh orange, tomato, and kiwi samples. The results showed excellent correlation (≥99 %) with gold-standard LC-MS/MS analysis, validating the sensor's reliability for direct, on-site measurements. The device also exhibited strong intra- and inter-batch reproducibility (RSD < 5 %) and reusability (up to 18 measurements per sensor). With an estimated manufacturing cost of only €0.32, the platform presents a robust, low-cost, and sustainable solution for real-time quality monitoring. Its versatility supports future adaptation for detecting additional compounds such as pesticides and sugars, advancing on-field diagnostics in agriculture and food safety.

1. Introduction

The global food industry faces increasing challenges related to food authentication, quality assurance, and safety monitoring including detection complexity, storage monitoring and supply risk chains lowering the consumer trust [1]. The assessment of quality in fruits and vegetables, as well as the monitoring of pesticide residues, storage conditions, and contamination, has gained significant attention due to

* Corresponding authors.
E-mail addresses: panagiota.kalligosfyri@unina.it (P.M. Kalligosfyri), stefano.cinti@unina.it (S. Cinti).
[1] These authors contributed equally.

https://doi.org/10.1016/j.electacta.2025.147285
Received 1 June 2025; Received in revised form 21 August 2025; Accepted 31 August 2025
Available online 2 September 2025

its implications for consumer health and agricultural sustainability [2]. Conventional methods for fruits and vegetables quality monitoring, primarily rely on chromatographic techniques. While these methods are known for their sensitivity and accuracy, they also come with significant drawbacks. They tend to require specialized personnel, increase analysis time due to lengthy pretreatment steps and raise costs because of the need for expensive equipment. Therefore, their use is often limited in decentralized areas. In contrast, portable sensors offer a promising alternative by enabling rapid, on-field testing. This capability supports timely decision-making for farmers, distributors, and quality inspectors, effectively bridging the gap created by traditional methods [3].

Electrochemical sensors offer significant advantages, enabling the realization of portable and robust devices tailored for on-site testing [3,4]. To this end, flexible platforms employing a variety of electrode fabrication materials including polydimethylsiloxane (PDMS) [5], polyester [6] and paper-based substrates [7] for screen-printed electrodes, have been engineered for pesticide detection on fruit and vegetable surfaces, ensuring practical and efficient monitoring solutions. In recent advancements, wearable glove sensors have been introduced, allowing direct analysis of pesticides on fruit peels [8,9] and leaves [10] without necessitating prior sample preparation, thus enhancing the feasibility of field-based testing.

Advancements in 3D-printing technology have introduced a promising alternative for electrochemical sensor fabrication. This technology enables the production of durable, customized electrodes, paving the way for integrated platforms capable of performing the entire analytical process from direct sampling without lengthy pretreatment steps to data interpretation on a laptop device or via a smartphone. A recent review highlights the successful incorporation of 3D-printed components, including electrodes, into the food quality control field [4,11,12].

3D printing enables the fabrication of electrodes with a wide variety of intricate and customizable surface patterns, allowing precise control over surface morphology to enhance electrochemical performance [13]. These electrodes can be configured with just a 3D-printed working electrode integrated into a system using external commercial electrodes, or fully 3D printed—with the working, counter, and reference electrodes all made from conductive polylactic acid (PLA). In the case of using solely 3D-printed working electrodes, this technology allows the creation of sensors with diverse surface geometries and material compositions, boosting their capacity to detect a wide range of analytes across complex matrices. Unique surface architectures, such as skyscraper-shaped geometry, have shown improved sensitivity and broader linear ranges [14]. A broad palette of materials, including carbon black/polylactic acid, multiwall carbon nanotube (MWCNT)/PLA, recycled PLA composites, graphene-based acrylonitrile butadiene styrene (ABS-G), and flexible carbon black/ thermoplastic polyurethane (TPU), has been explored to fine-tune performance for different analytical goals. For instance, early 3D-printed electrodes were used for mycotoxin detection in food [15], showcasing their potential in food safety. Similarly, a cost-effective and rapid dual-nozzle FDM method used ABS-G filaments to fabricate a tailored electrode for detecting the food contaminants, minimizing time and cost compared to commercial devices [16]. In the biomedical field, CB/PLA-based electrodes enabled ex vivo serotonin detection in the anorectum [17], while CB/PLA and MWCNT/PLA microelectrodes allowed for spatial serotonin mapping using standard redox probes [18]. The skyscraper design supported TNFα detection in fecal samples, revealing inflammation patterns associated with aging [14]. In another application, flexible CB/TPU electrodes allowed simultaneous detection of dopamine, uric acid, and nitrite in urine [19], showing promise for wearable diagnostics. In forensic screening, in-house fabricated recycled PLA/graphite/CB sustainable electrodes successfully detected ketamine in spiked beverages [20]. Altogether, these examples highlight the remarkable versatility of 3D-printed working electrodes not only in the materials and in-house fabrication strategies used, but also in their application across biomedical, environmental, food safety, and forensic domains. These partially 3D-printed electrochemical sensors, incorporating only 3D-printed working electrodes, already demonstrate enhanced performance through customizable designs and materials.

Fully 3D-printed sensors, however, take this flexibility even further by integrating all components, working, counter, and reference electrodes, into a single platform. This complete integration simplifies fabrication, enhances portability, and broadens application potential. For example, a fully 3D-printed nanozyme-enabled electrochemical sensor modified with Fe(II)-MOF, a metal-organic framework known for its electrocatalytic properties, enabled glucose detection in artificial sweat, offering a non-invasive tool for diabetes monitoring [21]. In neurological diagnostics, a fully 3D-printed electrode array was employed to detect Parkinson's disease biomarkers in blood and cerebrospinal fluid [22]. Another system, a dual microchip platform fabricated in a single print, enabled simultaneous detection of cardiac biomarkers (cholesterol and choline) from a single blood droplet [23]. Complementing these advances, another study demonstrated a fully 3D-printed electrochemical sensor with an integrated microwell for miRNA detection towards cancer diagnosis. Featuring precise fluid control, gold electrodeposition for surface modification, and picomolar-level sensitivity via methylene blue-labeled DNA probes, this platform underscores the versatility and diagnostic potential of 3D-printed sensing technologies in point-of-care settings [24].

Additionally, an innovative pre-treatment method based on the combination of photochemical and electrochemical oxidation processes to degrade excess binder material, enhanced the electrochemical properties of fully printed electrodes, allowing for low detection limits of metals like Cd(II) and Pb(II), pharmaceuticals such as midazolam, and biomolecules like uric acid [25]. These examples underline the growing potential of fully 3D-printed sensors to serve as powerful, self-contained diagnostic and monitoring tools, particularly in decentralized and field-deployable contexts.

Despite these advancements, the application of fully 3D-printed electrochemical sensors in on-site or in-field monitoring, such as in agriculture for assessing fruits, vegetables, and soil quality, remains underdeveloped, particularly when compared to the maturity of screen-printed sensors in terms of customizable designs and efficient material handling [4,11,12]. Nevertheless, the robustness, affordability, and adaptability of 3D-printed platforms offer a compelling opportunity to bridge this gap and enable real-time, decentralized sensing in field-based environments.

In this context, a novel fully 3D-printed sensor is presented for on-field fruit analysis, highlighting its innovative design, operational efficiency, and versatility in comparison to existing technologies. By leveraging conductive materials and customized fabrication through additive manufacturing, the sensor's design is optimized for portability, precision, and durability. A key feature is its trident shape that enables the direct insertion into fruit, eliminating the need for additional equipment, complex pre-treatment procedures, or extensive sample preparation, enabling real-time, accurate measurements. The lightweight, portable, and partially reusable sensor also supports easy, wireless connectivity between the 3D-printed electrodes and the potentiostat's connection pins, making it ideal for field applications in diverse agricultural environments. As a proof of concept, the sensor was applied to detect ascorbic acid (vitamin C) in oranges, kiwis and tomatoes, a compound linked to fruit and vegetables freshness and storage conditions [26,27]. This successful application highlights the sensor's potential for broader use for detecting various molecules in agricultural and food quality monitoring.

2. Materials and methods

2.1. Reagents and equipment

Potassium ferricyanide, ascorbic acid and all the other common reagents were obtained from Sigma-Aldrich (St. Louis, MO, USA). Silver/

Silver chloride conductive ink was used for the reference electrode realization (Loctite, Brugherio, Italy). The 3D-printed portable device (i.e. trident-shaped supporting part and electrodes) was printed using the Creality Ender-3 V2 Neo (Shenzhen Creality 3D Technology, Shenzhen, China). Protopasta conductive PLA filament 1.75 mm (Protoplant, Vancouver, WA, USA) was used for the fabrication of the 3D-printed electrodes, which was characterized previously [28]. The electrochemical measurements of the present work have been performed using the Emstat4S potentiostat (PalmSens, Houten, The Netherlands) connected to a laptop PSTrace 5.10 software.

2.2. Methods

2.2.1. Fabrication of the 3D-printed electrochemical sensor

A 3D-printed electrochemical sensor was integrated with a 3D-printed trident-shaped housing towards the realization of the ultimate, fully 3D-printed, sensing device. The 3D-printed electrodes were designed in the Autodesk Fusion design application with the following dimensions: 6 mm width, 2 mm thickness and 30 mm height. The design was then converted in the appropriate file format, i.e. Standard Tessellation Language (STL), and was inserted in the UltiMaker Cura 5.4.0, slicing application, to define the printing parameters: lines infill pattern with a 20 % infill density, printing speed at 70 %, nozzle temperature of 210 °C and printing bed temperature of 55 °C. The printing temperature used in the present study follows the manufacturer's recommendation, as lower temperatures resulted in clogging of the conductive filament, preventing successful electrode fabrication.

The reference electrode was created by applying a single-pass thin layer of silver/silver chloride (Ag/AgCl) conductive ink and was left to dry in room temperature for 30 min. The 3D-printed electrodes were inserted into the 3D-printed trident-shaped housing. Before use, the three-electrode system, comprising the working and counter electrodes made from conductive PLA filament and the Ag/AgCl reference electrode– was pretreated with a 0.5 M solution of NaOH [13,29]. A potential of 1.4 V was applied for 200 s, followed by a −1.0 V potential for another 200 s. Finally, the electrodes were rinsed with distilled water and were ready to use.

2.2.2. Electrochemical ascorbic acid detection

The 3D-printed trident-shaped device, consisting of a three-electrode system, was applied for the detection of ascorbic acid. After assembling the 3D-printed electrochemical sensing device, a calibration curve was constructed using standard solutions of ascorbic acid prepared in 10 mM ammonium acetate buffer (pH 4.7). The ascorbic acid concentrations ranged from 0 to 10 mM. The electrochemical response was recorded using linear sweep voltammetry (LSV), as the electrochemical technique, under the following experimental parameters: E begin:0.1 V, E end: +1.4 V, E step: 0.01 V, scan rate: 0.05 V/s.

2.2.3. Direct determination of ascorbic acid in fresh fruit sample using the fully 3D printed device

Following calibration, the 3D-printed trident-shaped device was used to directly measure ascorbic acid in a fresh fruit sample. The electrodes, integrated into the device, were inserted into the fruit, and the electrochemical measurements were performed under the LSV technique as described previously. The quantitative results were directly obtained from the fruit sample and interpreted using the calibration curve previously constructed in buffer solution.

2.2.4. Chromatographic determination of ascorbic acid

Preparation of standard solutions. Ascorbic acid stock solutions were prepared by weighing 10 mg of powder standard and solubilizing in 10 mL of milli-Q water containing 0,1 % formic acid, yielding a standard solution with a concentration of 1 mg/mL. Quantitative analysis was performed by construction of calibration curve using serial dilutions from stock solution.

LC–MS/MS instrumentation and conditions: 1µl of supernatant were analyzed by using a AB-sciex 5500 QTRAP® system with a HPLC chromatography system Exion LC™. The column used was Kinetex 5 µm C18 100 Å. The mobile phase was generated by mixing eluent A (0.1 % formic acid in water) and eluent B (0.1 % formic acid in methanol) and the flow rate was 0.200 mL/min. The chromatographic gradient was as follows: the mobile composition was maintained at 10 % of eluent B for 1 min, then eluent B was increased to 50 % and held for 2 min. Subsequently it was raised to 90 % eluent B for 2 min and finally returned in 10 % of eluent B for an additional 2 min for column equilibration.

The orange sample was peeled, the pulp coarsely shredded, and then placed in an 90:10 water/methanol (v/v) solution, following a shaking step in the dark for 3 h. Afterwards, the supernatant was collected, centrifuged for 10 min at 5000 rpm and filtered through 0.22 µm PTFE syringe filter. The resulting solution was then diluted and analyzed by tandem mass spectrometry in Multiple Reaction Monitoring mode.

3. Results and discussion

3.1. Configuration and assay principle of the 3D-printed trident-shaped device

A novel fully 3D-printed electrochemical sensor, integrated into a trident-shaped housing, as shown in Fig.S1A of the Supplementary Material, was developed for the determination of ascorbic acid. Designed using the Autodesk Fusion application, the electrodes were fabricated with conductive PLA filament, with dimensions of 6 mm width, 2 mm thickness, and 30 mm height (Fig.S1B). The device featured a three-electrode system (Fig.S1C): the working and counter electrodes were made from conductive PLA filament, while the reference electrode, also printed with conductive PLA, was coated with a thin layer of Ag/AgCl conductive ink. The 3D-printed housing for the electrodes was designed to facilitate the easy insertion of the sensing device into the fruit, penetrating the peel. Finally, the 3D-printed electrodes were easily inserted into the trident-shaped device through equally sized slits. For direct analysis of the ascorbic acid, known as vitamin C, in fresh oranges the pins of the electrodes were directly connected to the sensing device, as shown in Fig. 1.

The electrochemical detection of ascorbic acid was based on its oxidation to dehydroascorbic acid at the working electrode, which generated a measurable current proportional to the ascorbic acid concentration. The sensor was applied for ascorbic acid quantification in fresh fruit samples by directly inserting the trident-shaped device into the fruit (Fig. 1B). Results were analyzed using a calibration curve, demonstrating a direct and consistent correlation between ascorbic acid concentration and the electrochemical signal. The fully 3D-printed device was applied to various fruits and vegetables as proof of concept and to demonstrate the sensor's versatility and capabilities (Fig. 1C).

3.2. Optimization of the 3d-printed electrochemical sensor

Optimization studies were conducted to enhance the performance of 3D-printed electrodes and evaluate the new 3D-printed electrochemical sensor. These studies were focused on pre-treatment step utilizing various NaOH concentration, the electrodes' dimensions, and infill patterns to investigate their effect on the sensor's performance. Initially, cyclic voltammetry (CV) was used to evaluate the 3D-printed working electrode using 5 mM potassium ferricyanide in 1 M KCl. In the optimization studies of the 3D-printed working electrode, external screen-printed counter and reference electrodes, prepared as previously reported [30], were used for assessment.

3.2.1. Pre-treatment step

The pre-treatment step was examined in terms of varying NaOH concentration, due to the effect in electrochemical signal as referenced in previous studies [13,29]. Specifically, solutions without containing

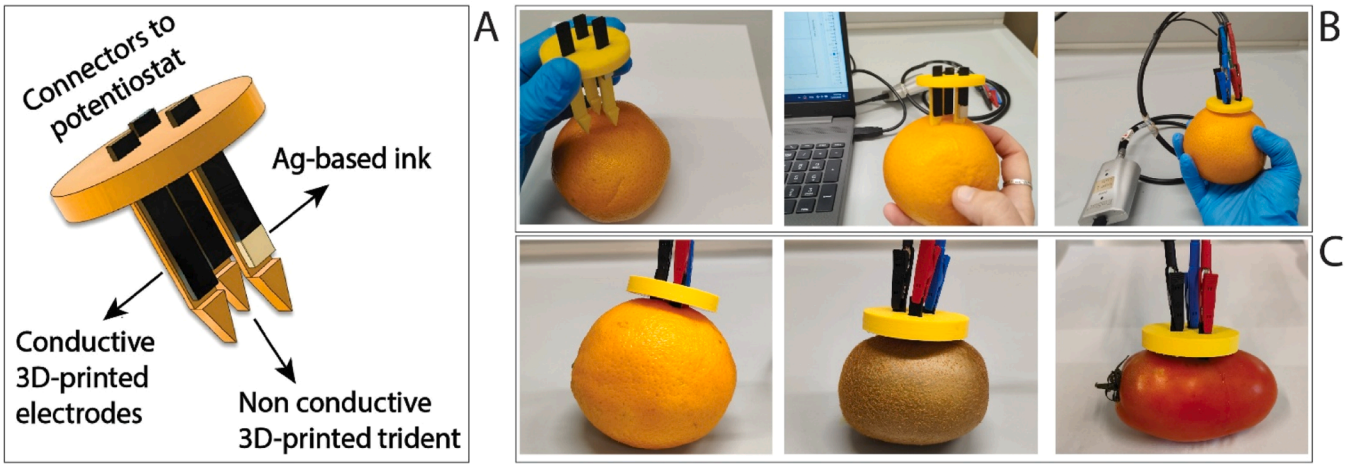

Fig. 1. A) Description of the trident-shaped 3D printed device, B) steps for implantation into fruit sample and connection to miniaturized and portable potentiostat for measurement, C) application of the trident-shaped 3D printed device to fruits and vegetables.

NaOH (0 M) and increasing concentrations of NaOH (0.1 M, 0.5 M, and 1 M) were evaluated for optimization.

SEM micrographs reveal notable differences in the surface morphology of 3D-printed electrodes before and after NaOH pretreatment. As shown in Figures S2A and S2B (non-pre-treated) compared to Figures S2E and S2F (pre-treated), the linear cavities in the line-patterned electrodes appear more continuous following the pretreatment process. Furthermore, when comparing Figures S2C and S2D (non-pre-treated) with S2G and S2H (pre-treated) at a smaller scale (300 μm), the NaOH treatment clearly creates deeper hollow regions within the electrode structure. This morphological transformation is attributed to the NaOH-induced release of the carbon component from the carbon-based PLA conductive filament, thereby enhancing the surface accessibility of the electrode [31,32]. This effect is not only visible in the SEM images but also supported by electrochemical measurements (Fig. 2A), where a 2.4-fold increase in current was observed when using the optimal NaOH concentration of 0.5 M.

Specifically, the application of the pretreatment step effectively doubled the electrochemical signal. Among the tested concentrations, 0.5 M NaOH provided the greatest signal enhancement, while increasing the concentration to 1 M did not result in any significant additional benefit.

This improvement in electrochemical performance can be attributed to the increased carbon load within the modified CB/PLA filament. The enhanced carbon content increases the likelihood of a higher density of electroactive sites and/or more efficient conductive pathways throughout the electrode, leading to better overall electron transfer kinetics and improved sensitivity [31].

3.2.2. *Dimensions*

The dimensions of the working electrode were identified as a critical parameter to investigate, as they can significantly influence the overall performance of an electrochemical sensor. The length and depth of the electrodes were fixed at 30 mm and 2 mm, respectively. The length of 30 mm was chosen to allow the insertion of the 3D-printed electrodes into samples of various sizes, leveraging the scalability offered by 3D-printing. The width, however, was systematically varied to determine its optimal value. The electrode widths were tested within the range of 2–10 mm. All electrodes were pre-treated with a 0.5 M NaOH solution and characterized using CV with a 5 mM potassium ferricyanide solution. The optimization studies were performed by registering the anodic and cathodic current density values and the characterization using varying scan rate from 0.02 to 0.5 V/s. The characterization graphs for all tested dimensions are provided in Fig. S3. As shown in Fig. 2B, a width of 6 mm for the working electrode produced the highest current density from 2 to 4 mm widths and the most consistent anodic and cathodic peaks, an essential feature in reversible systems such as potassium ferricyanide. In contrast, electrodes with widths of 8 mm and 10

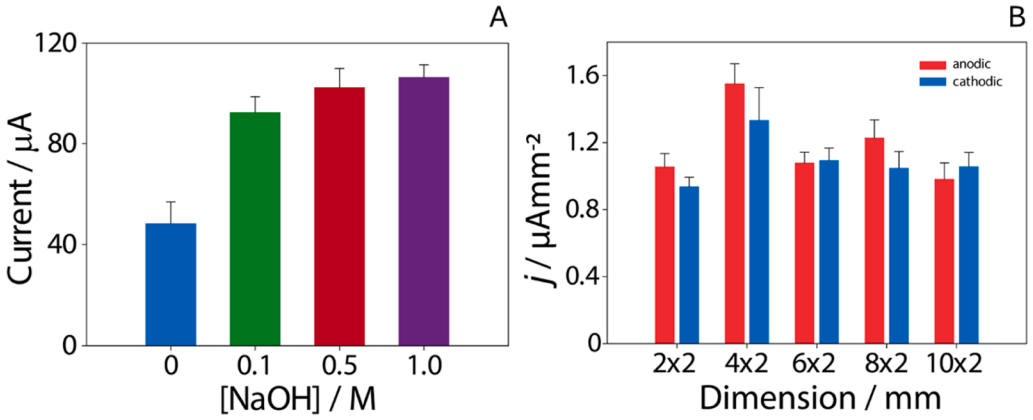

Fig. 2. A) NaOH pretreatment optimization evaluated at 0 (no pre-treatment), 0.1, 0.5 and 1.0 M concentration. The bars are obtained by monitoring the anodic current intensity peak recorded in CV at 0.05 V/s as scan rate, with a 5 mM $K_3Fe(CN)_6$ solution in 1 M KCl. B) Optimization of the 3D-printed working electrodes in varying width value keeping stable the thickness as 2 mm, evaluated at 2 × 2, 4 × 2, 6 × 2, 8 × 2 and 10×2 mm. The bars represent the anodic (red) and cathodic (blue) current density, with current intensities recorded in CV at 0.05 V/s as scan rate, with a 5 mM $K_3Fe(CN)_6$ solution in 1 M KCl. The experiments were performed in six replicates.

mm exhibited 20–40 % highest current than 6 mm, but less consistent anodic and cathodic peaks. Additionally, the 6-mm width required less printing time and material compared to the larger electrodes (Table S1). Consequently, the 6-mm width was selected not only for the working electrode but also for the counter and reference electrodes of the 3D-printed electrochemical sensor.

3.2.3. *Printing speed*

The printing speed during the 3D printing process was identified as an important parameter influencing the surface morphology and electrochemical performance of the fabricated electrodes [33,34]. In this study, printing speed was adjusted via the Cura slicer software, with 80 mm/s set as the baseline (100 % speed). The evaluated speed settings included 30 % (24 mm/s), 50 % (40 mm/s), 70 % (56 mm/s), and 100 % (80 mm/s). To assess the impact of printing speed on electrode surface characteristics, SEM analysis was conducted. At the lowest speed setting (30 %) (Fig. S4A and Fig. S4B), slower extrusion resulted in excessive material accumulation, particularly along the edges, leading to pronounced surface irregularities. These morphological features were especially evident at the 2 mm scale, where raised ridges and edge defects were observed. In contrast, electrodes printed at 50 % (Fig. S4C and Fig. S4D) and 70 % (Fig. S4E and Fig. S4F) exhibited a more uniform surface texture, with significantly smaller and more evenly distributed cavities. The highest speed setting (100 %, Fig. S4G and Fig. S4H) produced the most inconsistent and pronounced surface defects, which were highlighted in red in the corresponding SEM micrographs (Fig. S4).

Quantitative analysis using ImageJ software revealed median cavity diameters of 0.23 mm at 30 %, 0.09 mm at 50 %, 0.04 mm at 70 %, and 0.43 mm at 100 % printing speeds. These results demonstrate that a printing speed of 70 % (56 mm/s) produces the most homogeneous surface, minimizes edge defects, and improves electrode consistency, in agreement with previously reported findings[33]. This optimization is further validated by electrochemical measurements, which, although not yielding the highest current intensity 70 % speed demonstrated significantly more homogeneous voltammograms obtained from the 3D-pritned electrodes, within the same print batch (Fig. S5A), and reduced standard deviations (Fig. S5B). Together, these findings reinforce the selection of 70 % as the optimal printing condition for reliable and reproducible sensor fabrication.

3.2.4. *Infill patterns*

Various infill patterns available in the Cura slicer application, lines, cubic, gyroid, and cross3D (Fig. S6), were tested. These infill patterns were designed to create varied surface configurations on the electrodes, aiming to enhance the number of active sites available after NaOH pretreatment. SEM characterization was conducted to observe the morphology of the 3D-printed electrodes fabricated with different infill patterns (Fig. S7). The electrodes with different infill patterns were also characterized using CV in the presence of 5 mM potassium ferricyanide in 1 M KCl at various scan rates (Fig. S8). As shown in Fig. 3A, the lines and gyroid patterns produced the highest current responses. However, the gyroid configuration demonstrated poor reproducibility, making it unsuitable for consistent use. Interestingly, our results revealed that the simplest surface pattern, based on a basic line architecture, provided the most reproducible electrochemical responses (Fig. 3A).

Although more complex infill patterns with increased surface roughness and cavities initially appeared promising due to higher current densities, they ultimately led to inconsistencies that negatively affected sensor performance. This outcome is consistent with observations in literature, where enhanced sensitivity is often offset by poor reproducibility due to irregular or non-uniform surface features[35].

Notably, despite the inherent design flexibility of 3D printing, most studies to date have continued to replicate conventional, flat electrode geometries, rather than fully leveraging the “freedom of design” offered by additive manufacturing[35–37]. To truly harness the potential of 3D printing in electrochemical and electroanalytical applications, it is essential to move beyond conventional paradigms and focus on understanding and working within the constraints of printed materials.

In line with this perspective, our study showed that the use of a simple linear infill pattern, while structurally modest, demonstrated superior repeatability and performance, reinforcing the idea that thoughtful, material-aware design is more impactful than mere complexity.

While 3D printing offers unique opportunities for customizing electrode architecture and integrating electrochemical sensing directly into field-ready formats, our findings highlight a critical trade-off between sensitivity and reproducibility. Specifically, although more complex infill patterns tend to enhance current responses due to increased surface area and mass transport effects, they also introduce structural irregularities and printing inconsistencies that negatively impact measurement repeatability particularly in real-world samples such as fresh fruit, where heterogeneous matrices and variable insertion conditions amplify these effects. Interestingly, our study found that a simple linear infill pattern, though less architecturally intricate, delivered superior

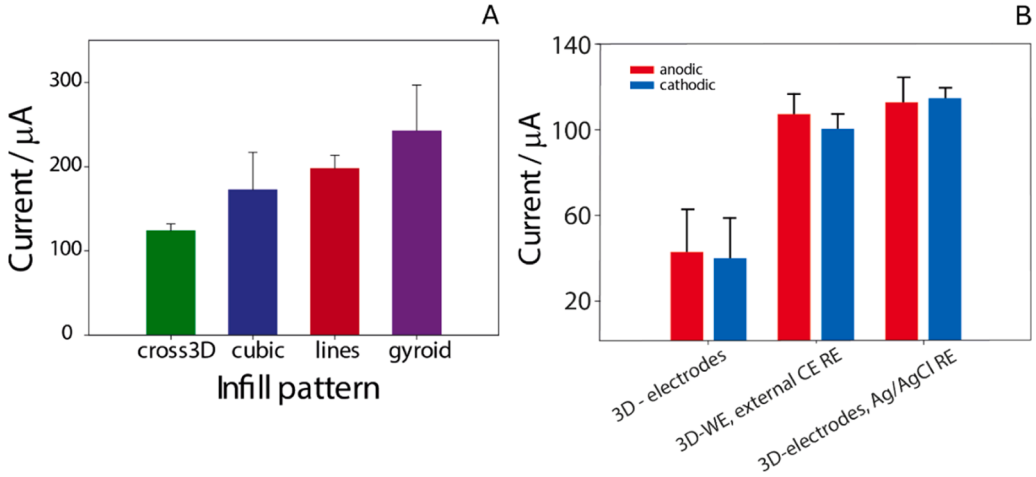

Fig. 3. A) Optimization of the 3D-printed working electrodes in varying infill patterns: cross3D, cubic, lines, gyroid bars B) Optimization of the three-electrode configuration: WE, CE and RE electrodes are 3D-printed (left), only the WE is 3D-printed while the CE and RE are external and screen-printed (middle) and the WE, CE and RE electrodes are 3D-printed but the RE is obtained by painting a section of the 3D printed electrode with Ag/AgCl conductive ink. The bars represent the anodic (red) and cathodic (blue) current intensity peaks recorded in CV at 0.05 V/s as scan rate, with a 5 mM $K_3Fe(CN)_6$ solution. The experiments were performed in six replicates.

consistency and electrochemical performance. This outcome reinforces the notion that practical sensor design benefits more from material-aware optimization than from geometric complexity alone[35]. As 3D printing technologies continue to advance, progress in this field will depend not only on exploring innovative designs but also on developing a deeper understanding of how fabrication parameters, material behavior, and functional stability converge to determine sensor reliability and applicability in complex environments.

3.2.5. Reference electrode investigation

The final device consisted of a 3D-printed, three-electrode system, with all electrodes having identical dimensions (6 × 2 × 30 mm) and utilizing the optimized lines infill pattern. Initially, the working electrode was tested alongside external counter and reference electrodes to validate its functionality. Once confirmed, measurements were performed using a fully 3D-printed system, where the working, counter, and reference electrodes were all fabricated from conductive PLA. To enhance sensor performance, the working electrode was first optimized, as described previously, and accordingly, the reference electrode was selected to match its size as the working area performance is directly associated with the signal response of the sensor [38]. After confirming the signal response of the 3D-printed electrochemical system, the reference electrode was further enhanced by applying a thin, single-pass layer of Ag/AgCl conductive ink (Fig. S9). This modification aimed to create a more stable and reliable three-electrode system, closely resembling the pseudo-reference electrode used in the initial evaluation of the 3D-printed working electrode. Additionally, this enhancement improved the reproducibility of the sensors, ensuring more consistent and accurate electrochemical measurements. The ultimate 3D-printed system, incorporating the coated reference electrode, was characterized and found to produce a response comparable to that of the external reference electrode, as shown in Fig. 3B

After completing the optimization studies, the final 3D-printed three-electrode sensor was characterized using potassium ferricyanide at varying scan rates (Fig. S10A and S10B). Additionally, potassium ferricyanide was employed as a model target to prepare a calibration curve in the concentration range of 0.05–1.00 mM. The system demonstrated good linearity, confirming its analytical performance (Fig. S10D).

3.3. Analytical performance of the 3D – printed trident-shaped electrochemical device

The optimized 3D-printed trident-shaped electrochemical device was analytically characterized by evaluating its performance in detecting ascorbic acid. A calibration curve for the ascorbic acid analyte was constructed using standard solutions prepared in 10 mM ammonium acetate buffer at pH 4.7, with analyte concentrations ranging from 0 to 5 mM. The electrochemical response was measured using LSV and the calibration curve was plotted by correlating the current response of the standard solutions with their respective concentrations. An increase in current was observed with higher concentrations of the target molecule, indicating a direct relationship between analyte concentration and electrochemical response. As shown in Fig. 4B, the sensor demonstrated good linearity within its linear detection range. Using the linear equation $y = 8.59x - 1.65$ ($R^2 = 0.99$), a limit of detection (LOD) of 0.130 mM was achieved, calculated according to the formula LOD = $3.3 \times \sigma_{blank}$ / m, where σ_blank is the standard deviation of the blank samples (0.330) and *m* is the slope of the calibration curve, while the limit of quantification (LOQ), calculated as LOQ = $10 \times \sigma_{blank}$ / m, was found to be 0.380 mM [39].

The 3D-printed electrochemical sensor developed in this work is compared to other methods (Table 1), emphasizing its performance and potential applications for on-field use. The performance of our fully 3D-printed electrochemical device highlights its effectiveness in detecting ascorbic acid in fresh fruits and vegetables, achieving a micromolar-level detection limit. This sensitivity is on par with that of screen-printed electrodes modified with nanoparticles, as well as commercial activated glassy carbon electrodes enhanced with graphene oxide-based nanocomposites [40,41]. Although such modified systems may reach lower limits of detection, they often involve costly materials and complex, time-consuming fabrication protocols [42–44]. In contrast, our sensor operates without any additional surface treatment, making it a more streamlined and cost-effective solution. A key advantage of our approach is the ability to perform direct measurements in whole samples as no solvents, extractions, or juice preparation are necessary [41,44,45]. This greatly reduces sample handling and allows for rapid, on-site analysis. To the best of our knowledge, this is the first report of a fully 3D-printed sensor being applied to ascorbic acid detection directly in fresh produce. Our device is uniquely designed in a trident shape for straightforward penetration into fresh samples, eliminating the need for any prior processing. This facilitates real-time, in situ measurements while offering benefits such as portability, structural durability, and low manufacturing costs. While some previously reported sensors may exhibit slightly higher sensitivity under optimized laboratory conditions, our platform excels in practical usability delivering a reliable, accessible, and field-ready solution for monitoring ascorbic acid in real food matrices.

The proposed approach is not restricted to LSV and can be readily extended to other electrochemical techniques, such as differential pulse voltammetry (DPV) or square wave voltammetry (SWV). SWV, in

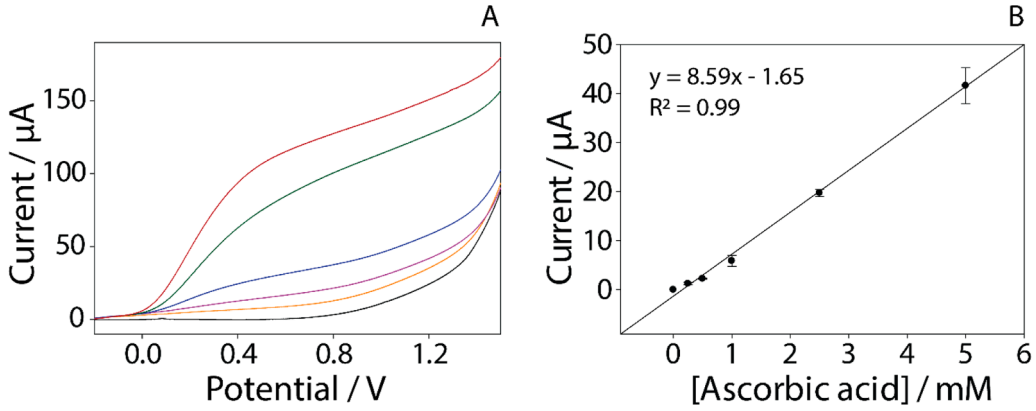

Fig. 4. A) Voltammetric curves obtained for increasing ascorbic acid concentrations. The black like represents the acetate buffer, that served as a blank sample, used to prepare the ascorbic calibrators. B) Calibration curve obtained at increasing concentrations of ascorbic acid (0–5 mM) in 10 mM of acetate buffer at pH 4.7. The 3D device responses were recorded in LSV in the potential range from −0.1 to +1.4 V at 0.05 V/s. The experiments were performed in six replicates. The non-linear baseline-corrected voltammograms are presented in Fig. S11 of the Supplementary File.

Table 1
Comparison of different electrochemical sensors for ascorbic acid detection across various samples and detection ranges. The table includes electrode type, method used, surface modifications, sample types, detection range, and limit of detection (LOD).

Electrode Type	Method	Surface Modification	Sample	Detection Range	LOD	Ref.
SPCE	SWV	*CV*-Fe_3O_4NP	10-fold diluted orange juice	0.010 – 0.10 mM	0.015 mM	[40]
AGCE	SWV	N/A	Garlic sample extracts	0.010 –0.20 mM	0.004 mM	[41]
SPE(a)	LSV	3D-rGO	2-fold diluted orange/ grape juice	1.0×10^{-5} –1.0×10^{-2} M	3.4×10^{-6} M	[42]
ITO-rGO-AuNPs electrode	LSV	rGO-AuNPs electrodeposition	Fruit juice	0.020–0.10 mM	0.006 mM	[43]
Inkjet-printed sensor	CV	CB	Dietary supplement	0–5 mM	0.15 mM	[46]
SPE	DPV	Gel-g-PS	Fresh fruit juices, vitamin C tablet	0.2–5 ppb and 20–600 ppb	0.03 ppb	[44]
GCE	CV	DMF/carboxyl/MWCNTs	Tomato sample extracts	1.0×10^{-6} to 1.0×10^{-3} M	2.5×10^{-7} M	[45]
3D-printed electrochemical sensor	LSV	N/A	Orange (in situ)	0–5 mM	0.13 mM	This work

SPCE: Screen-printed carbon electrode; SWV: square wave voltammetry; *CV*-Fe_3O_4NP: *Callistemon viminalis* iron(III) oxide nanoparticle; N/A: Nor applied, AGCE: activated glassy carbon electrode; SPE(a): active screen-printed electrode; 3D-rGO: three-dimensional graphene oxide; LSV: linear sweep voltammetry; ITO-rGO-AuNPs: indium tin oxide graphene oxide gold nanoparticles; CV: cyclic voltammetry; CB: carbon black; Gel-g-PS: gelatin grafted with poly sulfonamide derivative; DPV: differential pulse voltammetry; MWCNTs: carboxyl multiwalled carbon nanotubes.

particular, has been successfully applied in combination with fully 3D-printed sensors [24], demonstrating enhanced analytical performance in terms of sensitivity and peak resolution. These methods are therefore well suited for applications requiring more stringent quantitative analysis, especially in complex sample matrices.

3.4. Specificity studies

To evaluate the specificity of the sensor, interference studies were performed using common potential interferents for ascorbic acid electrochemical detection. Mercury (10 ppb) and copper (1 ppm) were selected based on their relevance in the literature [10], while glucose and citric acid (100 mM) were included to reflect to their presence in the sample matrix [46]. As shown in Fig. 5A, no significant interference peaks were observed at the peak potential of ascorbic acid, confirming the high specificity of the sensor for ascorbic acid detection in the presence of these interferents.

Even though the sensor already demonstrates good specificity for ascorbic acid in the presence of common interferents, future studies will evaluate its performance against a broader range of organic pesticides and insecticides to ensure reliability in more complex agricultural samples. The current results, however, confirm that the sensor performs well for ascorbic acid detection in fruit matrices, highlighting its suitability for immediate application. Expanding the specificity assessment in future work will further strengthen its applicability under more challenging and diverse sample conditions.

3.5. Determination of ascorbic acid in fruits and vegetables samples

To evaluate the accuracy and reliability of the fully 3D-printed electrochemical sensor, its performance was compared against the gold-standard Liquid Chromatography-Tandem Mass Spectrometry (LC-MS/MS) technique. Fresh fruit and vegetable samples (orange, tomato, and kiwi) were procured from the same vendor, originating from a single batch and stored under identical conditions to ensure consistency. Both methods were applied to analyze these samples.

Representative voltammograms obtained by LSV using the 3D-printed sensor for orange juice are presented in Fig. 5; additional voltammograms for tomato and kiwi are provided in the Supplementary material (Fig. S12). The ascorbic acid (AA) concentrations quantified by both techniques are summarized in Table S2.

The sensor yielded AA concentrations of 0.91 ± 0.02 mM (orange), 0.73 ± 0.06 mM (tomato), and 2.47 ± 0.20 mM (kiwi), closely aligning with LC-MS/MS results of 0.90 ± 0.09 mM, 0.63 ± 0.01 mM, and 2.58 ± 0.03 mM, respectively. The Pearson correlation coefficient (r) between the mean values from both methods was approximately 0.99, indicating a strong correlation between the two methods. The associated p-value of 0.021 indicates a statistically significant correlation, with only a 2.1 % probability that this strong agreement occurred by chance. These results substantiate the high analytical accuracy, precision, and reproducibility of the fully 3D-printed sensor for in situ quantification of ascorbic acid in complex fruit matrices, demonstrating its practical suitability for decentralized food quality monitoring.

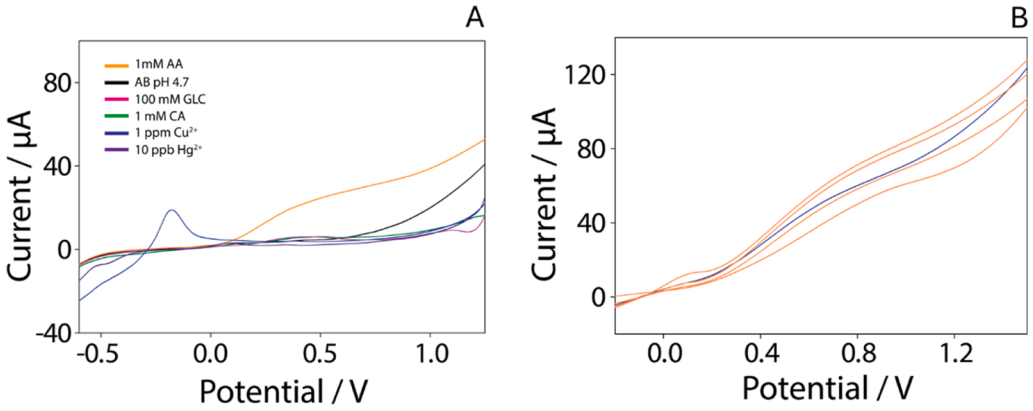

Fig. 5. A) Specificity study of the fully 3D-printed sensor. Mercury (Hg^{2+}), copper (Cu^{2+}), glucose (GLC) and citric acid (CA) were selected as potential interferents in the detection of ascorbic acid (AA). B) Voltammograms obtained using the fully 3D-printed device in the inside of the orange sample (orange line). In blue line is represented the voltammogram of the 1 mM of standard ascorbic acid solution for comparison. The 3D device responses were recorded in LSV in the potential range from −0.1 to +1.4 V at 0.05 V/s. The experiments were performed in four replicates.

3.6. Robustness and reusability of the fully 3D-printed sensor

Our fully 3D-printed sensor offers a sustainable, field-ready alternative by enabling direct analysis without reagents or sample prep, reducing chemical waste and time. While some lab-optimized sensors may show higher sensitivity, our device prioritizes usability, speed, and on-site testing for real-world food monitoring.

To assess the repeatability and reproducibility, key features for next-generation sensors, we performed electrochemical measurements using potassium ferricyanide on 16 electrodes fabricated across four independent 3D-printing batches ($n = 4$ electrodes per batch). As shown in Fig. S13A, the voltammograms are generally consistent, with only minor variations observed among some 3D-printed electrodes. Fig. S13B presents the corresponding peak current intensities and standard deviations, further supporting the reproducibility of the fabrication process. Specifically, Batches 1 and 2 exhibited low internal variability, indicating good repeatability, while Batches 3 and 4 showed slightly higher variation. A one-way ANOVA yielded a p-value of 0.39, indicating no statistically significant difference between the batches. Since $p > 0.05$, failure to reject the null hypothesis suggests that all batch means are statistically equivalent.

The 3D-printed sensor shows strong reproducibility and repeatability, with minor variations likely due to random factors. Its consistent performance and scalable fabrication make it ideal for reliable, real-world, on-field sensing applications.

Finally, regarding robustness and stability the reusability of the device was investigated. Up to three pretreatment steps were applied on the 3D-printed electrodes before proceeding with ascorbic acid detection at three different concentration levels, along with a blank sample. The detailed procedure can be found in the supplementary material. Each reuse cycle included the full process: cleaning, pretreatment, and analyte detection. Each 3D-printed sensor was used for up to six consecutive measurements and could be reactivated with NaOH pretreatment for three cycles, allowing a total of 18 uses while maintaining reproducibility and signal stability.

To evaluate the reusability of the electrodes, up to three reuse cycles were conducted, with ascorbic acid detection performed at three concentrations: 0.25 mM, 0.50 mM, and 1 mM. The results demonstrate the excellent reusability of the electrodes, with reliable performance maintained across all three cycles (Fig. S14). This indicates that the electrodes can be reused multiple times without significant loss of efficiency or sensitivity, supporting sustainability by reducing waste and the need for new electrodes in each analysis. The ability to reuse the electrodes up to three times significantly reduces both costs and environmental impact compared to traditional single-use sensors. This reusability factor highlights the sustainable nature of our device, minimizing material consumption and waste generation.

4. Conclusions

Based on the need for decentralized, low-cost, and real-time sensing solutions, we developed a fully 3D-printed electrochemical sensor tailored for on-field ascorbic acid detection in fruits and vegetables. The simple trident-shaped electrode design, optimized through careful control of printing parameters, proved to be the most effective in terms of signal stability, reproducibility, and ease of direct insertion into fresh samples. The customized trident electrode geometry, enabled by 3D printing, was specifically designed to meet the practical demands of direct fruit insertion for on-field ascorbic acid sensing. While such non-circular shapes may introduce edge effects and asymmetric diffusion, these factors were considered and do not compromise sensor reproducibility or performance under controlled conditions [35]. This tailored design represents a valuable advantage of additive manufacturing for application-specific electrochemical sensors.

The fully 3D-printed sensor enabled real-time analysis in orange, tomato, and kiwi samples, without requiring any sample pre-treating, showing a strong correlation with LC-MS/MS ($r \approx 0.99$), confirming analytical accuracy and reliability. It achieved a comparable detection limit to existing electrochemical systems, strong intra- and inter-batch reproducibility (RSD < 5 %) and demonstrated reusability for up to 18 measurements with 3 pre-treatment cycles per electrode. With a total cost of just €0.32 (€0.16 for reusable housing and €0.16 for electrodes), the device is an accessible and scalable solution for food quality monitoring. Its direct integration with portable platforms supports instant data acquisition and interpretation, eliminating the need for laboratory equipment.

The versatile design of our sensor can be extended beyond ascorbic acid to enable on-field detection of various analytes such as reducing sugars, pesticides, and pathogenic bacteria [47,48]. Both enzyme-based and enzyme-free electrochemical sensors modified with biomimetic nanomaterials have demonstrated high sensitivity for in situ sugar detection, while tailored electrode surfaces enable rapid pesticide monitoring under field conditions. Moreover, gold modification on 3D-printed electrode surfaces offers versatile immobilization strategies, paving the way for ready-to-use, application-specific sensors [24].

Although 3D-printed electrochemical sensors are still emerging and currently lag behind more established portable platforms, our goal is to close this gap by developing practical, low-cost, and multifunctional tools for real-time agricultural and food safety monitoring [12,49]. Key limitations such as fabrication reproducibility, material-dependent variability, and limited environmental stability, have hindered broader adoption of 3D-printed sensors [12,50].

In this work, we addressed several of these challenges by optimizing the 3D printing process, selecting durable, low-cost materials, and designing a simple, yet effective electrode geometry tailored for direct fruit insertion. This approach ensured consistent sensor performance, even in heterogeneous sample matrices, and supported reusability under field conditions. Additionally, we highlight the potential for future enhancement through integrated surface modifications, as previously reported [24], to improve sensitivity and selectivity without compromising cost or portability.

By targeting key challenges in design simplicity, fabrication consistency, and material robustness, our work demonstrates the practical viability of fully 3D-printed sensors as sustainable, field-ready solutions for decentralized food quality monitoring.

CRediT authorship contribution statement

Martina Tuccillo: Writing – original draft, Investigation. **Panagiota M. Kalligosfyri:** Writing – review & editing, Writing – original draft, Validation, Supervision, Methodology, Investigation, Formal analysis, Conceptualization. **Antonella Miglione:** Writing – review & editing, Writing – original draft, Validation, Methodology. **Concetta Di Natale:** Writing – review & editing, Writing – original draft, Validation, Methodology, Investigation, Formal analysis. **Michele Spinelli:** Writing – review & editing, Writing – original draft, Methodology, Investigation, Formal analysis. **Angela Amoresano:** Writing – review & editing, Writing – original draft, Supervision, Methodology, Formal analysis. **Donato Calabria:** Writing – review & editing, Writing – original draft, Methodology. **Mara Mirasoli:** Writing – review & editing, Writing – original draft, Methodology. **Ibrahim A. Darwish:** Writing – review & editing, Project administration. **Stefano Cinti:** Writing – review & editing, Writing – original draft, Supervision, Project administration, Methodology, Formal analysis, Conceptualization.

Declaration of competing interest

None

Acknowledgement

S.C. acknowledges the Pathogen Readiness Platform for “CERIC-

ERIC Upgrade" PRP@CERIC è finanziato dal PNRR Piano Nazionale di Ripresa e Resilienza nell'ambito della Missione 4 "Istruzione e Ricerca", Componente 2 "Dalla Ricerca all'Impresa", Linea di Investimento 3.1 "Fondo per la realizzazione di un sistema integrato di infrastrutture di ricerca e innovazione", finanziato dall'Unione Europea – Next Generation EU. PRIN project No 2022WN89PC entitled "Biomimetic sensing platforms for the detection of Alzheimer's disease related biomarkers" is acknowledged. The authors extend their appreciation to the Researchers Supporting Project number (RSPD2025R944), King Saud University, Riyadh, Saudi Arabia, for funding this work.

Supplementary materials

Supplementary material associated with this article can be found, in the online version, at doi:10.1016/j.electacta.2025.147285.

Data availability

Data will be made available on request.

References

[1] A. Haider, S.Z. Iqbal, I.A. Bhatti, M.B. Alim, M. Waseem, M. Iqbal, A. Khaneghah, Food authentication, current issues, analytical techniques, and future challenges: a comprehensive review, Compr. Rev. Food Sci. Food Saf. 23 (2024), https://doi.org/10.1111/1541-4337.13360.
[2] I. Vågsholm, N.S. Arzoomand, S. Boqvist, Food Security, safety, and sustainability—Getting the trade-offs right, Front. Sustain. Food Syst. 4 (2020) 16, https://doi.org/10.3389/fsufs.2020.00016.
[3] B. Brunetti, Electrochemical sensors and biosensors for the determination of food nutritional and bioactive compounds: recent advances, Sensors 24 (2024) 6588, https://doi.org/10.3390/s24206588.
[4] J. Xia, W. Huang, X. Wang, Z. Zhu, M. Zhang, X. Zhang, Flexible sensing technology for fruit quality control in the cold chain: characterization, application, and improvement, Food Control 154 (2023) 109976, https://doi.org/10.1016/j.foodcont.2023.109976.
[5] F. Zhao, J. He, X. Li, Y. Bai, Y. Ying, J. Ping, Smart plant-wearable biosensor for in-situ pesticide analysis, Biosens. Bioelectron. 170 (2020) 112636, https://doi.org/10.1016/j.bios.2020.112636.
[6] S.C. Teixeira, N.O. Gomes, M.L. Calegaro, S.A.S. Machado, T.V. de Oliveira, N. de Fátima Ferreira Soares, P.A. Raymundo-Pereira, Sustainable plant-wearable sensors for on-site, rapid decentralized detection of pesticides toward precision agriculture and food safety, Biomater. Adv. 155 (2023) 213676, https://doi.org/10.1016/j.bioadv.2023.213676.
[7] T.S. Martins, S.A.S. Machado, O.N. Oliveira, J.L. Bott-Neto, Optimized paper-based electrochemical sensors treated in acidic media to detect carbendazim on the skin of apple and cabbage, Food Chem. 410 (2023) 135429, https://doi.org/10.1016/j.foodchem.2023.135429.
[8] R.K. Mishra, L.J. Hubble, A. Martín, R. Kumar, A. Barfidokht, J. Kim, M. M. Musameh, I.L. Kyratzis, J. Wang, Wearable flexible and stretchable glove biosensor for on-site detection of organophosphorus chemical threats, ACS. Sens. 2 (2017) 553–561, https://doi.org/10.1021/acssensors.7b00051.
[9] A. Raucci, A. Miglione, G. Manganiello, C. Cimminella, L. Moio, S.L. Woo, J. Wang, S. Cinti, Sensing at your fingertip: on-glove electrochemical sensor for copper detection on vine leaves, ECS. Sens. Plus. 3 (2024) 044601, https://doi.org/10.1149/2754-2726/ad7da1.
[10] A. Miglione, A. Raucci, M. Mancini, V. Gioia, A. Frugis, S. Cinti, An electrochemical biosensor for on-glove application: organophosphorus pesticide detection directly on fruit peels, Talanta 283 (2025) 127093, https://doi.org/10.1016/j.talanta.2024.127093.
[11] D.J.S. Agron, W.S. Kim, 3D Printing technology: role in safeguarding food security, Anal. Chem. 96 (2024) 4333–4342, https://doi.org/10.1021/acs.analchem.3c05190.
[12] P. Kalligosfyri, A. Miglione, S. Cinti, Screen-printing and 3D-printing technologies in electrochemical (Bio)sensors: opportunities, advantages and limitations, ECS. Sens. Plus. 4 (2024) 010601, https://doi.org/10.1149/2754-2726/ada395.
[13] C. Miller, O. Keattch, R.S. Shergill, B.A. Patel, Evaluating diverse electrode surface patterns of 3D printed carbon thermoplastic electrochemical sensors, Analyst 149 (2024) 1502–1508, https://doi.org/10.1039/D3AN01592K.
[14] K.K. Hussain, R. Hopkins, M.S. Yeoman, B.A. Patel, 3D printed skyscraper electrochemical biosensor for the detection of tumour necrosis factor alpha (TNFα) in faeces, Sens. Actuators. B Chem. 410 (2024) 135694, https://doi.org/10.1016/j.snb.2024.135694.
[15] M. Zafir Mohamad Nasir, F. Novotný, O. Alduhaish, M. Pumera, 3D-printed electrodes for the detection of mycotoxins in food, Electrochem. Commun. 115 (2020) 106735, https://doi.org/10.1016/j.elecom.2020.106735.
[16] F.A. Arris, D. Mohan, M.S. Sajab, Facile synthesis of 3D printed tailored electrode for 3-monochloropropane-1,2-diol (3-MCPD) sensing, Micromachines 13 (2022) 383, https://doi.org/10.3390/mi13030383.
[17] H.H. Hamzah, O. Keattch, M.S. Yeoman, D. Covill, B.A. Patel, Three-dimensional-printed electrochemical sensor for simultaneous dual monitoring of serotonin overflow and circular muscle contraction, Anal. Chem. 91 (2019) 12014–12020, https://doi.org/10.1021/acs.analchem.9b02958.
[18] Z. Xue, K. Patel, P. Bhatia, C.L. Miller, R.S. Shergill, B.A. Patel, 3D-Printed microelectrodes for biological measurement, Anal. Chem. 96 (2024) 12701–12709, https://doi.org/10.1021/acs.analchem.4c01585.
[19] A.C.M. Oliveira, E. Bernalte, R.D. Crapnell, M.J. Whittingham, R.A.A. Muñoz, C. E. Banks, Advances in additive manufacturing for flexible sensors: bespoke conductive TPU for multianalyte detection in biomedical applications, Appl. Mater. Today 42 (2025) 102597, https://doi.org/10.1016/j.apmt.2025.102597.
[20] M.M.C. Souza, R.G. Rocha, G.P. Siqueira, R.D. Crapnell, E.M. Richter, C.E. Banks, R.A.A. Muñoz, Additively manufactured ready-to-use platform using conductive recycled PLA for ketamine sensing, Microchim. Acta 192 (2025) 60, https://doi.org/10.1007/s00604-024-06902-3.
[21] E. Koukouviti, A.K. Plessas, V. Pagkali, A. Economou, G.S. Papaefstathiou, C. Kokkinos, 3D-printed electrochemical glucose device with integrated Fe(II)-MOF nanozyme, Microchim. Acta 190 (2023) 274, https://doi.org/10.1007/s00604-023-05860-6.
[22] C. Kalinke, P.R. De Oliveira, C.E. Banks, B.C. Janegitz, J.A. Bonacin, 3D-printed immunosensor for the diagnosis of Parkinson's disease, Sens. Actuators. B Chem. 381 (2023) 133353, https://doi.org/10.1016/j.snb.2023.133353.
[23] E. Koukouviti, C. Kokkinos, 3D printed enzymatic microchip for multiplexed electrochemical biosensing, Anal. Chim. Acta 1186 (2021) 339114, https://doi.org/10.1016/j.aca.2021.339114.
[24] P.M. Kalligosfyri, C. Miller, S. Cinti, B.A. Patel, 3D printed electrode-microwell system: a novel electrochemical platform for miRNA detection, Microchim. Acta 192 (2025) 330, https://doi.org/10.1007/s00604-025-07190-1.
[25] H.A. Silva-Neto, M. Santhiago, L.C. Duarte, W.K.T. Coltro, Fully 3D printing of carbon black-thermoplastic hybrid materials and fast activation for development of highly stable electrochemical sensors, Sens. Actuators. B Chem. 349 (2021) 130721, https://doi.org/10.1016/j.snb.2021.130721.
[26] C.S. Johnston, D.L. Bowling, Stability of ascorbic acid in commercially available orange juices, J. Am. Diet. Assoc. 102 (2002) 525–529, https://doi.org/10.1016/S0002-8223(02)90119-7.
[27] N. Martí, P. Mena, J.A. Cánovas, V. Micol, D. Saura, Vitamin C and the role of citrus juices as functional food, Nat. Prod. Commun. 4 (2009) 677–700, https://doi.org/10.1177/1934578×0900400506.
[28] I.V.S. Arantes, R.D. Crapnell, E. Bernalte, M.J. Whittingham, T.R.L.C. Paixão, C. E. Banks, Mixed graphite/carbon black recycled PLA conductive additive manufacturing filament for the electrochemical detection of oxalate, Anal. Chem. 95 (2023) 15086–15093, https://doi.org/10.1021/acs.analchem.3c03193.
[29] E.M. Richter, D.P. Rocha, R.M. Cardoso, E.M. Keefe, C.W. Foster, R.A.A. Munoz, C. E. Banks, Complete additively manufactured (3D-Printed) electrochemical sensing platform, Anal. Chem. 91 (2019) 12844–12851, https://doi.org/10.1021/acs.analchem.9b02573.
[30] A. Raucci, M. Metitiero, C. Cuzzi, P.M. Kalligosfyri, M. Messina, M. Spinelli, A. Amoresano, S.L. Woo, I. Cacciotti, S. Cinti, Remediate-and-sense: alginate beads empowered by portable electrochemical strips towards copper ions removal and detection in environmental sites, Analyst 149 (2024) 3302–3308, https://doi.org/10.1039/D4AN00494A.
[31] R.S. Shergill, B.A. Patel, Preprinting saponification of carbon thermoplastic Filaments provides ready-to-use electrochemical sensors, ACS. Appl. Electron. Mater. 5 (2023) 5120–5128, https://doi.org/10.1021/acsaelm.3c00862.
[32] P.L. dos Santos, V. Katic, H.C. Loureiro, M.F. dos Santos, D.P. dos Santos, A.L. B. Formiga, J.A. Bonacin, Enhanced performance of 3D printed graphene electrodes after electrochemical pre-treatment: role of exposed graphene sheets, Sens. Actuators. B Chem. 281 (2019) 837–848, https://doi.org/10.1016/j.snb.2018.11.013.
[33] R.S. Shergill, B.A. Patel, The effects of material extrusion printing speed on the electrochemical activity of carbon black/polylactic acid electrodes**, ChemElectroChem. 9 (2022) e202200831, https://doi.org/10.1002/celc.202200831.
[34] R.G. Rocha, D.L.O. Ramos, L.V. de Faria, R.L. Germscheidt, D.P. dos Santos, J. A. Bonacin, R.A.A. Munoz, E.M. Richter, Printing parameters affect the electrochemical performance of 3D-printed carbon electrodes obtained by fused deposition modeling, J. Electroanal. Chem. 925 (2022) 116910, https://doi.org/10.1016/j.jelechem.2022.116910.
[35] W.B. Veloso, T.R.L.C. Paixão, G.N. Meloni, The current shortcomings and future possibilities of 3D printed electrodes, Anal. Chem. 96 (2024) 14315–14319, https://doi.org/10.1021/acs.analchem.4c02127.
[36] N. Rohaizad, C.C. Mayorga-Martinez, F. Novotný, R.D. Webster, M. Pumera, 3D-printed Ag/AgCl pseudo-reference electrodes, Electrochem. Commun. 103 (2019) 104–108, https://doi.org/10.1016/j.elecom.2019.05.010.
[37] A. Abdalla, B.A. Patel, 3D Printed electrochemical sensors, Annu. Rev. Anal. Chem. 14 (2021) 47–63, https://doi.org/10.1146/annurev-anchem-091120-093659.
[38] J. Krejci, Z. Sajdlova, V. Nedela, E. Flodrova, R. Sejnohova, H. Vranova, R. Plicka, Effective surface area of electrochemical sensors, J. Electrochem. Soc. 161 (2014) B147–B150, https://doi.org/10.1149/2.091406jes.
[39] G.L. Long, J.D. Winefordner, Limit of detection A closer look at the IUPAC definition, Anal. Chem. 55 (1983) 712A–724A, https://doi.org/10.1021/ac00258a724.
[40] G.E. Uwaya, O.E. Fayemi, Electrochemical detection of ascorbic acid in orange on iron(III) oxide nanoparticles modified screen printed carbon electrode, J. Clust. Sci. 33 (2022) 1035–1043, https://doi.org/10.1007/s10876-021-02030-7.

[41] D. Yenealem, D. Eyayu, D. Tibebe, M. Mulugeta, Y. Kassa, Z. Moges, F. Kerebih, T. Fentie, A. Amare, M. Ayalew, Electrochemical characterization and detection of ascorbic acid in garlic using activated glassy carbon electrode: a comprehensive study, Food Anal. Methods 17 (2024) 1473–1483, https://doi.org/10.1007/s12161-024-02660-3.

[42] E. Buffon, N.R. Stradiotto, Disposable three-dimensional graphene oxide electrode with sandwich-like architecture for the determination of ascorbic acid in fruit juices, Mater. Today Commun. 35 (2023) 105535, https://doi.org/10.1016/j.mtcomm.2023.105535.

[43] F. Mazzara, B. Patella, G. Aiello, A. O'Riordan, C. Torino, A. Vilasi, R. Inguanta, Electrochemical detection of uric acid and ascorbic acid using r-GO/NPs based sensors, Electrochim. Acta 388 (2021) 138652, https://doi.org/10.1016/j.electacta.2021.138652.

[44] H.S. Magar, A.M. Fahim, M.S. Hashem, Accurate, affordable, and easy electrochemical detection of ascorbic acid in fresh fruit juices and pharmaceutical samples using an electroactive gelatin sulfonamide, RSC. Adv. 14 (2024) 39820–39832, https://doi.org/10.1039/D4RA06271J.

[45] B. He, J. Zhang, Electrochemical determination of vitamin C on glassy carbon electrode modified by carboxyl multi-walled carbon nanotubes, Int. J. Electrochem. Sci. 10 (2015) 9621–9631, https://doi.org/10.1016/S1452-3981(23)11205-3.

[46] S. Cinti, N. Colozza, I. Cacciotti, D. Moscone, M. Polomoshnov, E. Sowade, R. R. Baumann, F. Arduini, Electroanalysis moves towards paper-based printed electronics: carbon black nanomodified inkjet-printed sensor for ascorbic acid detection as a case study, Sens. Actuators. B Chem. 265 (2018) 155–160, https://doi.org/10.1016/j.snb.2018.03.006.

[47] J. Xue, K. Mao, H. Cao, R. Feng, Z. Chen, W. Du, H. Zhang, Portable sensors equipped with smartphones for organophosphorus pesticides detection, Food Chem. 434 (2024) 137456, https://doi.org/10.1016/j.foodchem.2023.137456.

[48] Q. He, B. Wang, J. Liang, J. Liu, B. Liang, G. Li, Y. Long, G. Zhang, H. Liu, Research on the construction of portable electrochemical sensors for environmental compounds quality monitoring, Mater. Today Adv. 17 (2023) 100340, https://doi.org/10.1016/j.mtadv.2022.100340.

[49] C. Kokkinos, 3D-printed thermoplastic sensors for electrochemical biosensing, Curr. Opin. Electrochem. 51 (2025) 101699, https://doi.org/10.1016/j.coelec.2025.101699.

[50] R.M. Cardoso, C. Kalinke, R.G. Rocha, P.L. dos Santos, D.P. Rocha, P.R. Oliveira, B. C. Janegitz, J.A. Bonacin, E.M. Richter, R.A.A. Munoz, Additive-manufactured (3D-printed) electrochemical sensors: a critical review, Anal. Chim. Acta 1118 (2020) 73–91, https://doi.org/10.1016/j.aca.2020.03.028.